Sensitization of TiO2 with Aluminum Phthalocyanine: Factors Influencing the Efficiency for Chlorophenol Degradation in Water under Visible Light

ARTICLE *in* THE JOURNAL OF PHYSICAL CHEMISTRY C · JULY 2009

Impact Factor: 4.77 · DOI: 10.1021/jp9016882

Sensitization of TiO_2 with Aluminum Phthalocyanine: Factors Influencing the Efficiency for Chlorophenol Degradation in Water under Visible Light

Qiong Sun and Yiming Xu*

Department of Chemistry, Zhejiang University, Hangzhou, Zhejiang 310027, China

Received: February 24, 2009; Revised Manuscript Received: May 15, 2009

Aluminum tetracarboxyphthalocyanine adsorbed on TiO_2 has been examined as a sensitizer for degradation of 4-chlorophenol (4-CP) in water under visible light irradiation ($\lambda \geq 450$ nm). It was observed that 4-CP was mostly decomposed into CO_2 and chloride ions, whereas the reaction rate was greatly influenced by several parameters. The optimum loading of the dye on TiO_2 was about 1.0 wt %, nearly independent of TiO_2 used. The solution pH which favored 4-CP degradation over the dye loaded TiO_2 was about pH 7. An increase in 4-CP concentration below 0.27 mM resulted in increased rate of 4-CP degradation, the kinetics well fitted into the Langmuir−Hinshelwood equation. In the flow of N_2, the reaction was almost completely inhibited. Experiments through EPR spin trapping, methanol quenching, and silver ions as electron acceptors revealed the involvement of superoxide, hydroxyl and dye cation radicals in the dye sensitized reaction. Evidence is well interpreted in terms of the electron transfer from the excited dye to TiO_2, followed by generation of the reactive species. However, among different sensitizers, the observed difference in activity is hardly correlated with their differences in the particle size, surface area, crystalline structure, and crystallinity of bare TiO_2, and in the dye absorbance and aggregation as well, whereas it is well in accordance with the trend in pore volume, measured for these samples through O_2 adsorption−desorption at 77 K. The result demonstrates for the first time the predominant role of O_2 to the dye sensitized degradation of organic pollutants over TiO_2 in aqueous suspension. Furthermore, the dye loaded TiO_2 under visible light was also active for degradation of other aromatic pollutants such as sulfosalicylic acid, from which the dye cation radical with a redox potential of about 1.25 V vs NHE at pH 6.5 is inferred.

Introduction

Titanium dioxide has been widely studied as a semiconductor photocatalyst for potential application in air purification and water treatment.[1−3] Various reactive species have been found in the UV irradiated TiO_2 system, including conduction band electrons (e_{cb}^-), valence band holes (h_{vb}^+), superoxide radicals ($O_2^{-\bullet}$), hydroxyl radicals ($^\bullet OH$), and singlet molecular oxygen ($^1O_2$).[4] These species have different redox potentials (−0.5 to +2.7 V vs NHE at pH 6.5),[4] and thus they can make almost all organic pollutants degraded into small fragments and/or carbon dioxide. However, due to a wide band gap of TiO_2 (3.2 eV), the reaction only occurs on the excitation with UV light, which is expensive, and/or only accounts for about 5% of solar light reaching the Earth's surface. Also, due to fast recombination of charge carriers, the quantum yield for organic degradation is usually very low. For example, a reliable quantum yield, obtained by using a blackbody like reactor for phenol oxidation in the aqueous suspension of TiO_2 (Degussa P25) at pH 3, is only 0.14 at 365 nm.[5]

Metallophthanlocyanines (MPc) are a class of macrocyclic complexes that have intensive absorption in the visible region. Many studies have shown that MPc and its derivatives are good sensitizers for generation of $^1O_2$ via energy transfer (eqs 1 and 2).[5,6] The sensitization reactions thus have been applied successfully for degradation of substituted phenols, sulfide, and methyl Orange either in a homogeneous solution or on an inert adsorbent such as silica, polymers and organoclay.[6−13] The dye pigments have been also used for spectral sensitization of TiO_2, so as to improve the efficiency in dye-sensitized solar cell,[14−16] and in water treatment.[17−26] For example, Litter and co-workers have shown that aluminum tricarboxymonoamidephthalocyanine can be chemically linked to the surface of TiO_2 via ester bond, and the immobilized dye on TiO_2 is an efficient sensitizer for organic oxidation in water under visible light irradiation.[18] They have proposed that the adsorbed dye on TiO_2 can inject electrons from its excited states into the conduction band of TiO_2, followed by generation of the dye cation radical ($dye^{\bullet+}$) and $O_2^{\bullet-}$. Since the $dye^{\bullet+}$ radical has a redox potential of about 1.2 V vs. NHE,[5,18] it can oxidize a suitable substrate (R), together with recovery of the original dye (eqs 2−5). In this cycle, TiO_2 only acts as an electron mediator, and the dye as a sensitizer. From an environmental point of view, such the dye sensitized system may be useful for treatment of recalcitrant pollutants such as chlorophenols.[18−21] However, little work has been made about the influencing factors, such as the physical properties of TiO_2. Also, the active species involved in the process have not been clearly demonstrated.

$$\text{dye} + h\nu \rightarrow \text{dye}^* \quad (1)$$

$$\text{dye}^* + O_2 \rightarrow \text{dye} + {}^1O_2 \quad (2)$$

$$\text{dye}^* + TiO_2 \rightarrow \text{dye}^{\bullet+} + TiO_2(e_{cb}^-) \quad (3)$$

$$TiO_2(e_{cb}^-) + O_2 \rightarrow TiO_2 + O_2^{\bullet-} \quad (4)$$

$$\text{dye}^{\bullet+} + R \rightarrow \text{dye} + R^{\bullet+} \quad (5)$$

In this work, several TiO_2 samples with different physical properties have been studied as a support of aluminum tetra-

* To whom correspondence should be addressed. Phone: +86-571-87952410. Fax: +86-571-87951895. E-mail: xuym@css.zju.edu.cn.

10.1021/jp9016882 CCC: $40.75
Published on Web 06/12/2009

TABLE 1: Physical Parameters for Commercial TiO_2 Samples[a]

samples	An (%)	I (cps)	d_s (nm)	S_{BET} (m^2/g)	d_p (nm)	V_p (cm^3/g)
CAT	97	1 322	12.6	137	16.7	0.622
CPT	84	2 392	25.0	51	14.6	0.185
CRT	92	3 056	31.1	46	19.0	0.240

[a] Values for An, anatase phase content; I, peak intensity; d_s, crystallite size, obtained from XRD; S_{BET}, BET surface area, d_p, pore size; V_p, pore volume, measured from N_2 adsorption at 77 K.

carboxyphthalocyanine. Their sensitization activities under visible light irradiation ($\lambda \geq 450$ nm) were evaluated by using degradation of 4-chlorophenol in aqueous solution as a model reaction. Several parameters were considered, including the dye loading on TiO_2, the substrate concentration, the solution pH, and the amount of O_2 present. Possible involvement of $dye^{\bullet+}$, $O_2^{\bullet-}$, and $^{\bullet}OH$ radicals in the dye sensitized reaction were examined through silver ions as electron acceptors, and through electron paramagnetic resonance spectroscopy in the presence of DMPO as spin traps. The composite sensitizers were characterized by powder X-ray diffraction, UV−visible reflectance spectroscopy, and adsorption−desorption isotherms of N_2 or O_2 at 77 K. Moreover, the dye loaded TiO_2 was also used for degradation of other aromatic pollutants with different redox potentials, from which the oxidizing ability of $dye^{+\bullet}$ radical may be estimated. The result shows that the dye sensitized reaction is in agreement with the pathways as previously proposed (eqs 1−5), but the catalyst capacity toward O_2 adsorption in aqueous solution is a predominant factor, as compared with others, such as the crystalline structure of TiO_2, and the aggregation of the adsorbed dye on TiO_2.

Experimental Section

Materials. Three commercial samples of TiO_2 were used as received, named as CPT (Degussa P25), CAT, and CRT (both from Taixing Nanomaterials, China), respectively. These oxides have different physical parameters (Table 1), as obtained from XRD and N_2 adsorption−desorption at 77 K (Figures S1 and S2 in the Supporting Information). Aluminum 2,9,16,23-tetracarboxyphthalocyanine (AlPcTC) was synthesized and purified as previously described,[27−29] using $AlCl_3$ and trimellitic anhydride as precursors. The analogue complexes of ZnPcTC, CuPcTC and CoPcTC were also prepared by a similar procedure. All chemicals were in analytical grade, including phenol, 4-chlorophenol (4-CP), 2,4-dichlorophenol (2,4-DCP), 2,4,6-trichlorophenol (2,4,6-TCP), benzoquinone, hydroquinone, catechol, resorcinol, salicylic acid, 5-sulfosalicylic acid, and *N*,*N*-dimethylformamide (DMF). The DMPO reagent (5,5-dimethyl-1-pyrroline-*N*-oxide) was purchased from Sigma, and stored at −18 °C before use.

Immobilization of AlPcTC on TiO_2. All samples were prepared by following a similar procedure as described by Roman and co-workers.[18] A solution of AlPcTC in DMF at a desirable concentration was added into aqueous suspension of TiO_2 (1.25 g/L) under magnetic stirring. After shaking overnight, the particles were collected through a membrane (pore diameter, 0.45 μm), washed thoroughly with water, and dried in a vacuum oven at 80 °C. The resulting green powder was then grounded in an agate-mortar, and stored in the dark. The amount of the adsorbed dye on TiO_2 was calculated by the change of dye concentration before and after adsorption, and expressed in units of weight percent (wt %) in the text.

Characterization and Analysis. Powder X-ray diffraction (XRD) patterns were recorded on a D/max-2550/PC diffractometer (Rigaku) using a Cu Kα as X-radiation source (40 kV; 300 mA). The phase content was estimated with the integrated intensities of anatase (101) and rutile (110). The corresponding crystallite size (d_s) was calculated using the Scherrer equation. The adsorption−desorption isotherm of N_2 or O_2 was measured at 77 K on a Micromeritics ASAP2020 apparatus. The Brunauer−Emmett−Teller surface area (S_{BET}) was calculated by the twelve-point method, and the pore volume (V_p) was estimated at $P/P_o = 0.99$ from the desorption branch. Diffuse reflectance spectra were recorded on a Varian Carry 500 Spectrophotometer using $BaSO_4$ as a reference. Infrared absorption spectra were recorded on a Nicolet 470 FTIR spectrophotometer with a KBr pellet.

Solution spectra were taken with an Agilent 8453 UV−vis spectrophotometer. Photoluminescence spectra were recorded on a Shimadzu RF-5301pc instrument. Electron paramagnetic resonance (EPR) spectra in the presence of DMPO were recorded at room temperature on a Bruker A300 spectrometer (microwave frequency, 9.78 GHz; microwave power, 20 mW; modulation amplitude, 1G). For all experiments, the same quartz capillary tubes were used as so to minimize the errors. Voltammetric experiments were performed on an electrochemical workstation (Chi660A, Shanghai Chenghua Instrument Corp) in a three-electrode compartment, using a platinum plate as working electrode, a platinum wire as counter electrode, and calomel electrode as reference. The measurement was made in aqueous solution containing 0.15 M Na_2SO_4, and 2.5 mM organic substrate. The scan rate was set at 50 mV s^{-1}. The redox potentials measured for phenol, 4-CP, 2,4-DCP, and 2,4,6-TCP in aqueous solution at pH 6.5 were 1.11, 1.00, 0.97, and 0.88 V vs NHE, which were very close to those reported by Li and Hoffman (1.06, 1.02, 0.96, and 0.87 V vs NHE, respectively).[30]

Organic substrates was analyzed by the standard method of high performance liquid chromatograph (HPLC) on a Dionex P680, equipped with an Apollo C18 reverse column (eluent, $CH_3OH:H_2O = 3:2$; flow rate, 1.0 mL/min; detection wavelength, 280 nm). Inorganic analysis was made by the standard method of ionic chromatograph (IC) on a Dionex ISC90, equipped with a conductivity detector and an AS14A column (eluent, 10 μM $Na_2CO_3/NaHCO_3$; flow rate, 1.0 mL/min).

Photosensitization. The irradiation source was a Halogen lamp (500 W) equipped with a cutoff filter at 450 nm. The reactor was a thermostatted Pyrex glass vessel (80 mL). Before irradiation, the aqueous suspension (50 mL) containing 1.0 g/L catalyst and 0.23 mM organic substrate was stirred for 30 min. At a given reaction time, 1.8 mL of the suspension was withdrawn, and filtered through a membrane (pore diameter, 0.22 μm). The filtrate was then analyzed by HPLC and IC.

Results and Discussion

AlPcTC Loaded onto Different Oxides. The dye easily adsorbed onto SiO_2, Al_2O_3, and TiO_2 from a DMF aqueous solution. No desorption was found by resuspension of the green powder in water. Their sensitization activities were then evaluated under visible light irradiation ($\lambda \geq 450$ nm), by using a model reaction of 4-CP degradation in an aerated aqueous solution at pH 5.5. Figure 1 shows the results for the catalysts loaded with 0.40 wt % AlPcTC. We see that the disappearance of 4-CP with irradiation time is only obvious with three dye loaded TiO_2 samples, whereas the reactions over the dye loaded SiO_2 and Al_2O_3 are both very slow. Control experiments in the dark, or under visible light irradiation with bare oxides showed negligible degradation of 4-CP. The result is similar to those

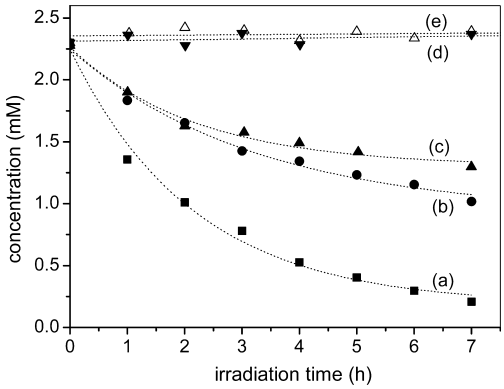

Figure 1. Photosensitized degradation of 4-CP in aerated aqueous suspension at pH 5.5 over 0.40 wt % AlPcTC-loaded oxides of (a) CAT, (b) CPT, (c) CRT, (d) SiO_2, and (e) Al_2O_3.

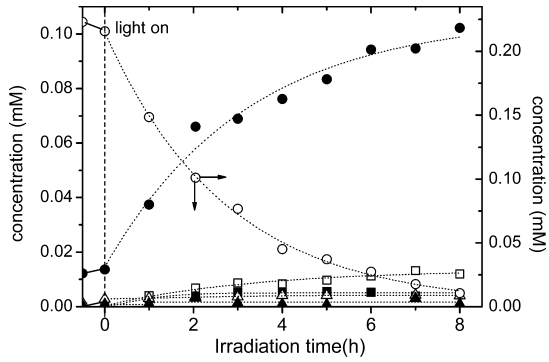

Figure 2. Concentration changes in solution as a function of irradiation time of 4-CP (○), Cl^- (●), HQ (■), BQ (□), formate (▲), and acetate (Δ), measured with 0.40 wt % AlPcTC-loaded CAT.

previously reported,[17−21] and confirms that as a support of sensitizer, TiO_2 is indeed superior to SiO_2 and Al_2O_3.

The photosensitized degradation of 4-CP on TiO_2-supported AlPcTC was also verified by monitoring the reaction intermediate or product with IC and HPLC techniques. Figure 2 shows the result obtained with 0.40 wt % AlPcTC-loaded CAT. The disappearance of 4-CP was indeed accompanied by a gradual formation of Cl^-, hydroquinone, benzoquinone, formate, and acetate. In relation to the consumed 4-CP in moles at 8 h, about 50% of chloride ions and 10% of organic species were formed in solution (note that data do not include the adsorbed products on TiO_2). Moreover, the suspension pH was also decreased to 3.5. The result suggests that 4-CP is mostly mineralized into CO_2 and Cl^- in the present system.

Roman and co-workers[31] have demonstrated that under visible light irradiation, the adsorbed AlPcTC on SiO_2 can generate $^1O_2$ via energy transfer (eq 2). However, the quantum yield of $^1O_2$ generation not only is lower than that measured with free dye in a homogeneous solution, but also decreases with the dye loading on SiO_2, due to increased dye aggregation. It is also known that 4-CP can react with $^1O_2$ to form benzoquinone, but the reaction is very slow at a pH lower than $pK_a = 9.41$ (the rate constants for 4-CP and its phenolate are 6.0×10^6 and 1.9×10^8 M^{-1} s^{-1}, respectively).[8a,32] Because of those reasons, little degradation of 4-CP was observed with the adsorbed dyes on SiO_2 and Al_2O_3. Then, the significant degradation of 4-CP observed with TiO_2-supported dye would be largely ascribed to other reactive species, such as $AlPcTC^{\bullet+}$ and $O_2^{\bullet-}$, presumably produced via electron transfer (eqs 3−5).

However, at the same dye loading (0.40 wt %), three TiO_2 samples display notably different activities for the dye sensitized

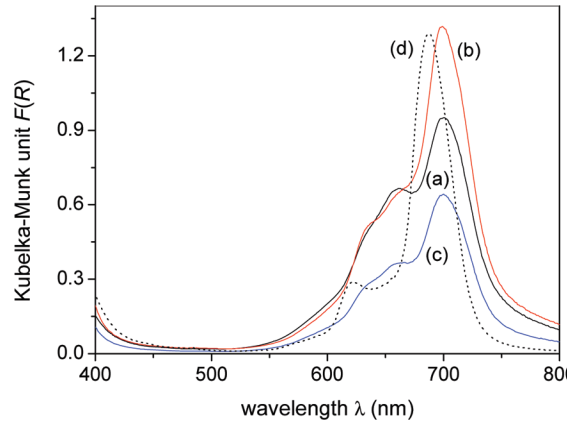

Figure 3. Visible diffuse reflectance spectra of 0.40 wt % AlPcTC loaded on (a) CAT, (b) CPT, and (c) CRT. The *y*-axis is expressed in the Kubelka−Munk unit, $F(R) = (1 - R)^2/2R$, where R is the reflectance. Curve (d) is the spectrum for the free AlPcTC dissolved in DMF (27 uM).

reaction (curves a-b, Figure 1). The relevant rate constants of 4-CP disappearance, obtained with CAT, CPT, and CRT-supported sensitizer, are $k_{obs} = 0.33$, 0.11, and 0.075 h^{-1}, respectively. Chen and co-workers have claimed that amorphous TiO_2 is better than crystalline TiO_2, for the CuPcTC sensitized degradation of methyl orange in water under visible light, ambiguously ascribed to a higher substrate adsorption onto the former.[21] In the present study, dark adsorption of 4-CP on the catalyst was negligible, even though the bare TiO_2 samples have different physical properties (Table 1). It implies that the observed difference among these samples is due to other factors, which will be discussed below.

First evidence emerges from the optical properties of these samples (Figure 3). In the visible light region, all samples display a wide absorption band centered at 700 nm. But their relative absorbance is obviously different, following the order of CPT > CAT > CRT. Moreover, these samples also show different degree of dye aggregation, as estimated by the absorbance ratio at 660 nm to that at 700 nm.[33] The blank TiO_2 only absorbs UV light (Figure S3 in the Supporting Information), whereas free AlPcTC in DMF has a narrowed monomer band at 687 nm (curve d, Figure 2). Then, the band broadening and red-shift observed with TiO_2-supported dye are characteristic of a specific interaction of the dye with the TiO_2 surfaces. In general, dye aggregation is not beneficial to the sensitization reaction, due to promoted deactivation of the dye excited states.[5,8,15,33] In this regard, the adsorbed dye on CPT should be the best sensitizer for 4-CP degradation, since it has the highest absorbance but the lowest dye aggregation among three samples. Unfortunately, this is not in agreement with the observation (Figure 1). Therefore, more studies are needed to clarify the role of TiO_2 in the dye sensitized reaction.

It was noted that ZnPcTC, CuPcTC, and CoPcTC loaded on CAT were also reactive for 4-CP degradation under visible light irradiation. However, ZnPcTC suffered a faster photobleaching than AlPcTC, whereas both CuPcTC and CoPcTC displayed a very low activity, as compared to AlPcTC and ZnPcTC. Moreover, under UV light irradiation, all of the dyes loaded on TiO_2 were quickly degraded, as previously reported.[26] Therefore, in this study, we only examine AlPcTC as a sensitizer under visible light.

Effect of Dye Loading on TiO_2. The composite catalysts were prepared under similar conditions only with different dye concentrations in DMF. Figure 4 shows the results of 4-CP

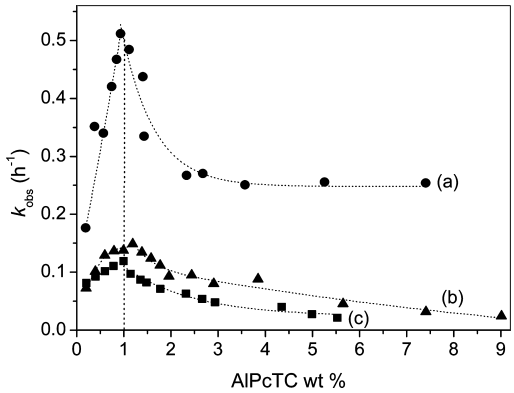

Figure 4. Effect of dye loading on (a) CAT, (b) CPT, and (c) CRT, on the apparent rate constant of 4-CP photodegradation in aerated aqueous suspension at pH 5.5.

oxidation obtained with these catalysts (1.00 g/L) in an aerated aqueous solution at pH 5.5. We see that the apparent rate constant of 4-CP loss first increases, and then decreases with the dye concentration on TiO_2. Interestingly, in spite of different TiO_2 used (Table 1), the optimal dye loading on each TiO_2 is almost the same (i.e., 0.93 wt % on CAT, 0.99 wt % on CRT, and 1.19 wt % on CPT). This is somewhat unexpected, since the reaction rate at a fixed incident light intensity should increase toward a plateau as the dye concentration is increased. No regular change of 4-CP adsorption on these catalysts was observed in the dark (the adsorption was only 1.2−3.6% of the total 4-CP added). Moreover, at any given dye loading, the relative activity of TiO_2 for the dye sensitized reaction always follows the order of CRT < CPT < CAT, similar to that observed above in Figure 1.

The rate decrease at high dye loading might be due to increased dye aggregation on TiO_2. For this concern, the reflectance spectra of these samples were recorded and analyzed. Figure 5 only shows the absorbance at 700 nm and at 660 nm as a function of dye loading. At first, we see that the absorbance does increase toward a plateau as the dye concentration on TiO_2 is increased. However, the normalized spectra (Figure S4 in the Supporting Information) show that as the dye loading on TiO_2 is increased, the dye aggregation on TiO_2 is decreased, not increased. Such a dye deaggregation even follows an increasing trend of CPT < CRT < CAT. Second, the adsorbed dye on CRT always has a lower absorbance than does the dye on CAT or CPT, whereas the dye on CAT only has a higher absorbance than that on CPT at a loading higher than 1.8 wt %. The reason for these unusual behaviors is not clear at the present. In general, the increase in light absorption and the decrease in dye aggregation should result in enhancement in the rate of dye sensitized reaction. But, such prediction is not always in accordance with the results (Figure 4), especially at a dye loading higher than 1.0 wt %. On the other hand, one may speculate that the dye in the form of dimer or higher-order aggregator, in relative to the monomeric dye, would have a higher efficiency in the electron injection to the conduction band of TiO_2. However, it is again not consistent with the observation that the dye on CRT is more aggregated than the dye on CPT (Figure S4 in the Supporting Information), but it always shows a lower photoactivity for the sensitized degradation of 4-CP (Figure 4). Therefore, it is difficult to make a reasonable conclusion only based on the above information in Figures 4 and 5.

It is noted that at the optimal dye loading, only small fraction of the surface sites of TiO_2 is covered with the dye (i.e., 6.9% on CAT, 26% on CPT, and 21% on CRT). This is estimated assume that each dye takes a flat orientation to the surface monolayer, and has a size dimension of $1.3 \times 1.1 = 1.4$ nm^2. The surface area that is occupied by the dye at 1.0 wt % is then calculated to be 11 m^2 per gram of TiO_2, which is much smaller than that area, measured with N_2 adsorption at 77 K (Table 1). This implies that most of the catalyst surfaces would be covered by substrates such as solvent and O_2.

Effect of O_2 and Detection of Reactive Species. The reaction was carried out with 1.0 wt % dye loaded samples, and the results are shown in Figure 6. We see that the rates of 4-CP loss measured in the presence of pure O_2 are all larger than those only in an air-equilibrated suspension. Second, in the atmosphere of pure N_2, the reactions are almost totally inhibited, but they can occur when $AgNO_3$ is present. No photodegradation of 4-CP in the aqueous solution of $AgNO_3$ was found under similar conditions. The result clearly demonstrates that the dye$^{\bullet+}$ radicals, produced through the electron transfer from the excited dye to TiO_2 (eq 3), are able to oxidize 4-CP present in the system (eq 5). Without electron scavenger, such as O_2 and Ag^+, the dye$^{\bullet+}$ radicals would recombine with the electrons on TiO_2, consequently resulting in null reaction with 4-CP.

We also see that the pure O_2 induced rate enhancement is notably different from one catalyst to another. For the dye loaded CAT, CPT, and CRT, the ratio of rate constant in the presence of O_2 to that in air is 1.33, 1.05, and 1.03, respectively. It implies that the catalyst capacity toward O_2 adsorption in water might be the main factor, responsible for their difference in activity for the dye sensitized oxidation of 4-CP. However, it is difficult to evaluate O_2 adsorption on these samples in solution. The measurement was then performed in a solid−gas phase through O_2 adsorption−desorption at 77 K (Figure S5 in the Supporting Information). For the dye loaded CAT, CPT, and CRT samples, the pore volume at $P/P_0 = 0.99$ was determined to be 0.592, 0.327, and 0.270 cm^3/g, respectively, whereas the corresponding BET surface area was 122, 44, and 41 m^2/g. Interestingly, the relative pore volume or surface area among these samples follows the same trend as that in the effect of O_2 on the dye sensitized degradation of 4-CP (Figure 6). This provides circumstantial evidence supporting our hypothesis. The catalyst with a higher pore volume would have more O_2 adsorbed onto it from aqueous solution. As a result, the back electron transfer from TiO_2 to dye$^{\bullet+}$ is retarded, and the oxidation of 4-CP by dye$^{\bullet+}$ is accelerated.

The reactive oxygen species were then examined through EPR in the presence of DMPO as a spin trap. Figure 7 shows the EPR spectra obtained with 1.0 wt % dye loaded catalysts. After visible light irradiation for 90 s, the sextet peaks of DMPO−$^{\bullet}$OOH/$O_2^{-\bullet}$ adduct in methanol aqueous suspension were observed with all samples (left column, Figure 7), whereas the quartet peaks of DMPO−$^{\bullet}$OH adducts were only notably found with CAT-supported sample (right column, Figure 7). Moreover, the EPR signals were somewhat decreased on the addition of 4-CP (curve b, Figure 7). No EPR signals were observed in the dark with all catalysts, and/or under visible light irradiation with bare TiO_2. The result confirms that $O_2^{\bullet-}$ is generated in the dye-loaded TiO_2 system (eq 4), followed by protonation into $HO_2^{\bullet}$ ($pK_a = 4.69$). Second reduction of $HO_2^{\bullet}/O_2^{\bullet-}$ by the electrons on TiO_2 would result in formation of $^{\bullet}$OH radicals. Such the reaction would be promoted when the catalyst has a high pore volume for uptake of O_2 from aqueous solution, such as CAT-supported sensitizer. The EPR result illustrates again that the catalyst capacity toward O_2 uptake in aqueous solution is the determining

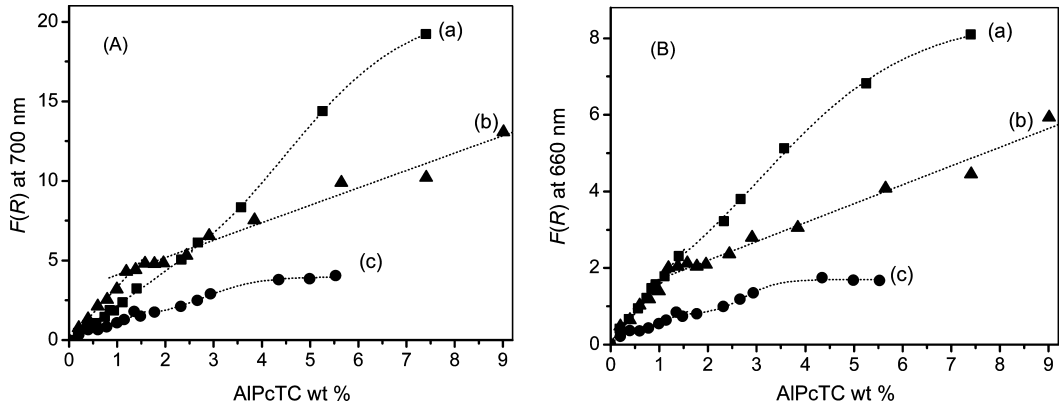

Figure 5. Specific absorbance of the catalysts at (A) 700 nm and (B) 660 nm as a function of dye loading on (a) CAT, (b) CPT, and (c) CRT.

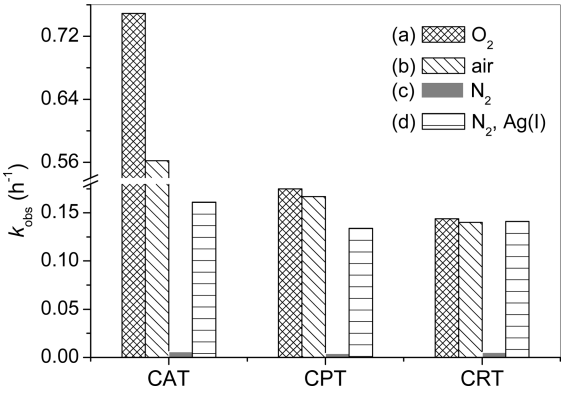

Figure 6. Apparent rate constant of 4-CP oxidation in water at pH 5.5, obtained with 1.0% AlPcTC loaded on CAT, CPT and CRT. The aqueous suspension was (a) bubbled with pure O_2, (b) open to air, (c) bubbled with pure N_2, and (d) bubbled with pure N_2 in the presence of $AgNO_3$ (0.10 mM).

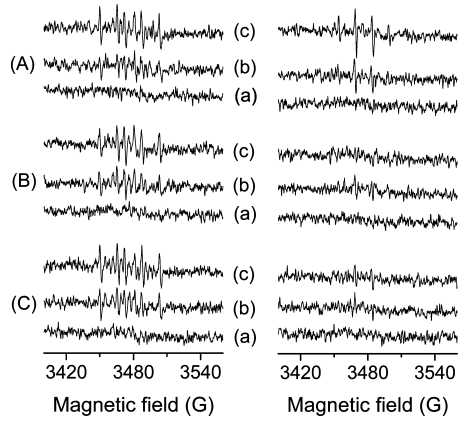

Figure 7. DMPO spin-trapping EPR spectra, recorded for superoxide radicals in 50% methanol (left), and for hydroxyl radials in water (right). The measurement was made with 1.0 wt % AlPcTC loaded on (A) CAT, (B) CPT, and (C) CRT, under different conditions of (a) 4-CP + catalyst + dark, (b) 4-CP + catalyst + visible light for 90 s, and (c) water + catalyst + visible light for 90 s.

factor for generation of reactive species, and consequently for degradation of target substrate at the solid−liquid interface.

The involvement of $^{\bullet}OH$ radicals in the dye sensitized oxidation of 4-CP was also evidenced by an quenching experiment with ethanol (note that the rate constants of ethanol and 4-CP with $^{\bullet}OH$ are 1.5×10^9 and 9.3×10^9 M^{-1} s^{-1}, respectively[34,35]). Figure 8 shows the results obtained with 1.0 wt % dye loaded catalysts in aerated aqueous suspension. On the addition of ethanol (50 mM), the rates of 4-CP oxidation

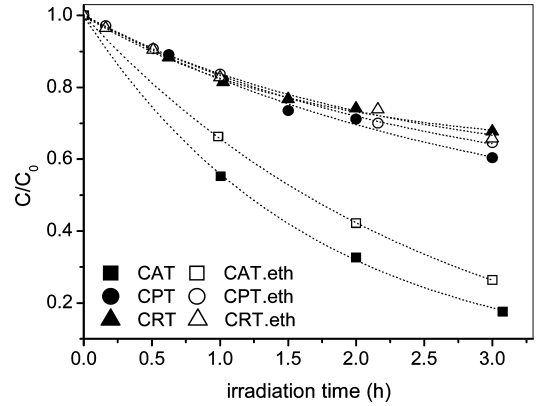

Figure 8. Effect of ethanol (eth, 50 mM) on the photosensitized oxidation of 4-CP in water at pH 5.5, measured with 1.0 wt % dye loaded CAT, CPT, and CRT, respectively.

are somewhat inhibited with all catalysts. But, such a rate decrease is more obvious with CAT-supported dye than those for the dyes on CPT and CRT, consistent with the EPR result in Figure 7.

Effect of Crystalline Structures. The commercial TiO_2 samples used above are in fact a mixture of anatase and rutile (Table 1). Among them, CAT has the highest value both in anatase phase content, and in activity for the dye sensitized degradation of 4-CP (Figure 4). Then, question may arise whether anatase is better than rutile for the dye sensitized reaction. For this concern, two TiO_2 samples in a form of pure anatase (SAT) and rutile (SRT) were separately synthesized according to literature procedure,[36] and characterized by XRD and O_2 adsorption−desorption at 77 K (Figures S6 and S7 in the Supporting Information). The solid was loaded with 1.0 wt % dye, and then used for 4-CP degradation in aerated aqueous suspension at pH 5.5. However, the result showed that the rate constant of 4-CP degradation over the dye loaded SAT was about twice smaller (0.031 h^{-1}) than that (0.096 h^{-1}) obtained with the dye loaded SRT. The relative activity between SAT and SRT for the dye sensitized reaction matches again the trend in pore volume (Table 2). Nevertheless, the observed difference in activity can not correlate with their differences in crystalline type, crystallinity, average particle size, and surface area, since the correlation is contrary to those made for commercial TiO_2 samples (Table 1 and Figure 4). Therefore, the catalyst sorption capacity toward O_2 from aqueous solution is the main factor that influences the relative activity of TiO_2 for the dye sensitized degradation of 4-CP.

Effect of pH. This experiment was performed with 1.0 wt % dye loaded CAT, and with the corresponding free dye in

TABLE 2: Physical Parameters Obtained for Synthetic TiO_2 Samples[a]

samples	I (cps)	d_s (nm)	S_{BET} (m^2/g)	d_p (nm)	V_p (cm^3/g)
SAT	2 726	4.1	152	2.5	0.096
SRT	5 777	11.0	38	19.9	0.188

[a] Notation are the same as in Table 1. The values for I and d_s are taken from XRD for anatase (101) and rutile (110). Values for S_{BET}, d_p, and V_p are calculated from O_2 adsorption−desorption isotherms at 77 K.

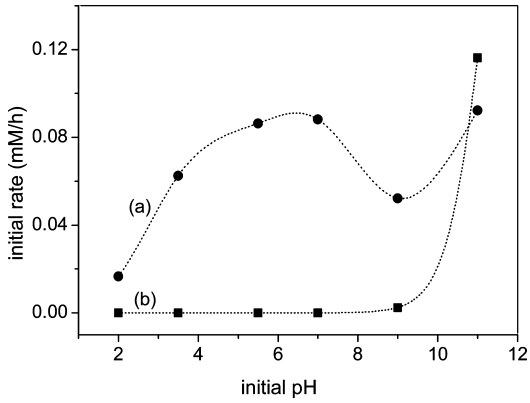

Figure 9. Effects of initial pH on the initial rate of 4-CP degradation in aerated aqueous solution, measured with (a) the free dye in solution (13 μM) and (b) 1.0 wt % dye loaded CAT.

solution as well. Figure 9 shows the initial rate of 4-CP disappearance as a function of initial pH. We see that the initial rates of 4-CP degradation over the dye loaded TiO_2 are always larger than those measured with the free dye in solution at pHs 2−9. The significantly high activity of the immobilized dye on TiO_2 is ascribed to its ability in generation of $AlPcTC^{\bullet+}$ and $HO_2^{\bullet}/O_2^{\bullet-}$, whereas the negligible rate with free dye in solution is due to very slow reaction of $^1O_2$ with 4-CP.

The reaction rate observed with the dye loaded TiO_2 also increases with the solution pH (curve b, Figure 9). This is roughly in accordance with the one-electron redox potential of 4-CP that decreases with increasing alkalinity in aqueous solution at a pH lower than pK_a = 9.37.[29] However, after reaching a limit at pH 7, the rate is first decreased at pH 9, and then increased again at pH 11. The former is ascribed to partial desorption of the adsorbed dye from TiO_2 surface, whereas the latter is due to fast reaction of $^1O_2$ with 4-CP anions. In an alkaline solution (1 M NaOH), complete dye desorption from TiO_2 was observed. Due to light scattering by the suspended TiO_2 particles, the number of incident photons available to the dye in solution is reduced, and thus the reaction rate is decreased, in relative to the reaction with free dye in a homogeneous solution. The result indicates that the composite sensitizer is only stable against dye desorption at a pH lower than 9.

Effect of 4-CP Concentration. The experiment was performed with 1.0 wt % dye loaded CAT at pH 5.5. Figure 10 shows the initial rate of 4-CP loss, R_0, as a function of the initial of 4-CP concentration, C_0. We see that R_0 first increases and then decreases slightly with C_0 (curve a, Figure 10). The kinetic data at $C_0 \le 0.27$ mM are well fitted into the Langmuir−Hinshelwood (L-H) equation, $R_0 = k_{LH}KC_0/(1 + KC_0)$, where k_{LH} and K are the rate constant and adsorption constant, respectively. The reciprocal plot of $1/R_0$ versus $1/C_0$ is satisfactorily linear (curve b, Figure 10), from which the corresponding parameters result, $k_{LH} = 0.168$ mM h^{-1}, and $K = 7.31$ mM^{-1}. This might be taken as the evidence of surface reaction between 4-CP and reactive species such as $AlPcTc^{\bullet+}$. The rate decrease at $C_0 > 0.27$ mM

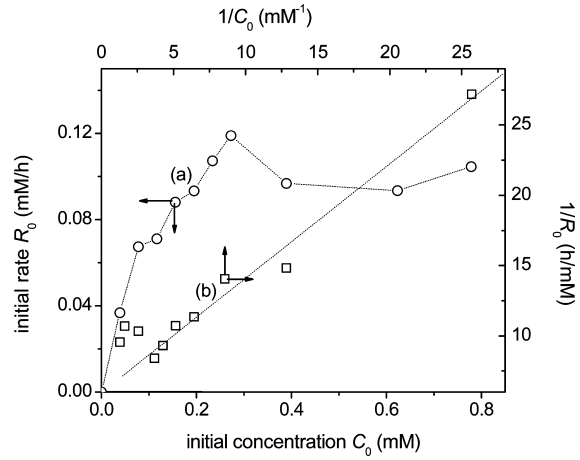

Figure 10. Effects of initial 4-CP concentration on the initial rate of 4-CP degradation, measured at pH 6.5 with 1.0 wt % dye loaded CAT. The curve (b) is the corresponding Langmuir−Hinshelwood plot.

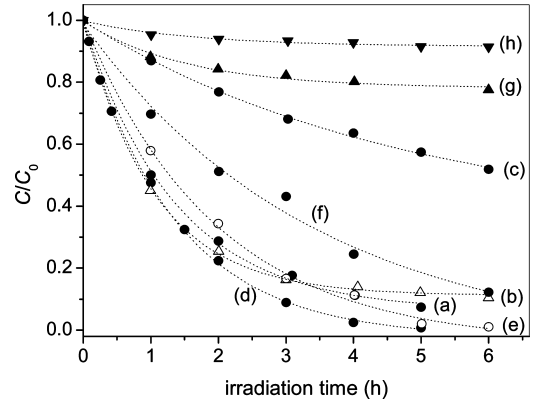

Figure 11. Photodegradation of different organic substrates (0.12−0.32 mM) in aerated aqueous suspension with 1.0 wt % dye loaded TiO_2. The substrates from (a) to (h) were phenol, hydroquinone, catechol, 4-CP, 2,4-DCP, 2,4,6-TCP, salicylic acid, and 4-sulfosalicylic acid.

might be due to promoted quenching of the excited dye by 4-CP, as evidenced by fluorescence experiment in DMF (the emission intensity at 704 nm due to the monomeric AlPcTC was decreased on the addition of 4-CP, Figure S8 in the Supporting Information).

Degradation of Different Organic Substrates. The dye loaded catalyst was also active for degradation of other aromatic substrates in aerated aqueous suspension under visible light irradiation. Figure 11 shows the results for several selected substrates with different redox potentials (0.33−1.25 V vs NHE at pH 6.5), including phenol, 4-CP, 2,4-DCP, 2,4,6-TCP, catechol, hydroquinone, salicylic acid, and 4-sulfosalicylic acid. We see that all substrates undergo a continuous degradation within irradiation time. In particular, 4-sulfosalicylic acid, that has a redox potential of 1.25 V vs NHE at pH 6.5, is also degradable (cure h, Figure 10). This provides circumstantial evidence that $AlPcTC^{\bullet+}$ has a redox potential of about 1.25 V vs NHE at pH 6.5, close to those previously reported (1.18 V for AlPc,[5] and 1.24 V for aluminum tricarboxymonoamidephthalocyanine[18]). In this regard, the dye loaded TiO_2 may find a wide application for organic degradation in water under visible light irradiation. Note that different rate of organic degradation in Figure 11 does not present the relative reactivity among different organic substrates, since these compound have different adsorption on the catalyst (data not shown).

Recycling Experiment. The catalyst stability is one of the important factors for practical application. Figure 12 shows the

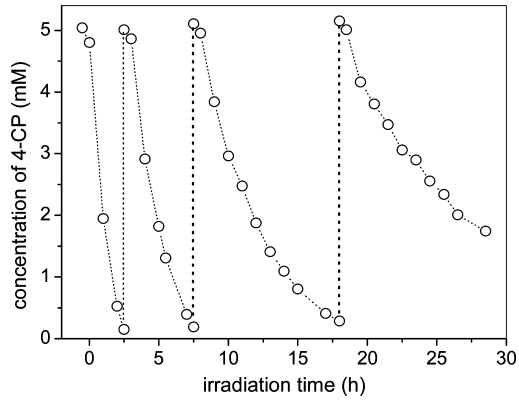

Figure 12. Recycling experiment for 4-CP degradation in the aerated aqueous suspension of 1.0 wt % dye loaded TiO_2 (2.0 g/L). After each run, the catalyst was collected, and redispersed into new solution of 4-CP, followed by equilibrium and light irradiation.

repeated experiments for 4-CP degradation with 1.0 wt % dye loaded TiO_2. We see that the rate of 4-CP photodegradation gradually decreases with the number of consecutive runs. Three causes are possible. First, the catalyst concentration decreases somewhat from one run to another, due to filtration and collection. Second, the intermediates formed from 4-CP degradation and adsorbed on the catalyst would compete with 4-CP for the reactive species generated from the irradiated catalyst. Third, the immobilized dye on TiO_2 suffers from a gradual bleaching during the photoreaction process. For this concern, the sample after the last run was collected and washed with 0.1 M NaOH. The dissolved dye in solution showed a similar absorption spectrum to that of unirradiated sample, but the absorbance at 682 nm was decreased by 25% (Figures S9 in Supporting Information). From these data, one may estimate the turnover number to be 712 (the degraded dye is 1.33 μmol, and the totally degraded 4-CP is 948 μmol). Control experiment in the absence of TiO_2 showed that only 1% of AlPcTC was bleached after the solution was continuously irradiated for 27 h. It means that the dye bleaching on TiO_2 is not due to the dye reaction with 4-CP and/or O_2, but it should be ascribed to decomposition of $AlPcTC^{\bullet+}$, generated from the irradiated catalyst (eq 3). In addition, FTIR analysis showed that the collected sample after the last run still displayed a similar spectrum as that of unirradiated sample, except new vibrations at 1210 and 1160 cm^{-1}, ascribed to hydroquinone adsorbed on TiO_2 (Figures S9 in the Supporting Information). It means that decarboxylation does not occur during the reaction (Figure 12), and the remaining dye is still in the form of AlPcTC.

Conclusions

This work has shown that aluminum phthalocyanine loaded on TiO_2 is a good sensitizer for degradation of substituted phenols in aerated aqueous solution under visible light irradiation. The reaction rate is greatly influenced by experimental parameters. Among the factors considered, such as the crystalline structure of TiO_2, the amount of O_2 adsorption on the composite sensitizer is predominant to the dye sensitized reaction. The optimal loading of dye on each of three TiO_2 supports is all about 1.0 wt %, which may imply a necessary balance between the amount of O_2 adsorbed and the number of photons absorbed, so as to achieve a maximal efficiency in organic degradation. The observed reaction is well interpreted in terms of the electron transfer from the excited dye to TiO_2. And the involvement of dye cation, superoxide and hydroxyl radicals are demonstrated through EPR and quenching experiments. However, the reason for the "unusual" effect of dye loading on the optical properties and sensitization activities of composite sensitizers still remains unclear. Further study is needed to clarify this issue.

Acknowledgment. This work is supported by the National Natural Science Foundation of China (Nos. 20477038, 20525724, and 20873124) and the National Basic Research Program of China (973 Program) (No. 2009CB825300). We thank Prof. Xuxu Wang at Fuzhou University and Dr. Run Liu at Zhejiang University for kind help with the diffuse reflectance and fluorescence spectrum measurement.

Supporting Information Available: XRD patterns, adsorption−desorption isotherms, diffuse reflectance, FTIR, and fluorescence spectra. This material is available free of charge via the Internet at http://pubs.acs.org.

References and Notes

(1) Ollis, D. F., Al-Ekabi, H., Eds.; *Photocatalytic Purification and Treatment of Water and Air*; Elsevier: Amsterdam, The Netherlands, 1993.
(2) Hoffmann, M. R.; Martin, S. T.; Choi, W.; Bahnemann, D. W. *Chem. Rev.* **1995**, *95*, 69–96.
(3) Carp, O.; Huisman, C. L.; Reller, A. *Prog. Solid State Chem.* **2004**, *32*, 33–177.
(4) Tachikawa, T.; Fujitsuka, M.; Majima, T. *J. Phys. Chem. C* **2007**, *111*, 5259–5275.
(5) Darwent, J. R.; Douglas, P.; Harriman, A.; Porter, G.; Richoux, M. C. *Coord. Chem. Rev.* **1982**, *44*, 83.
(6) DeRosa, M. C.; Crutchley, R. *Coord. Chem. Rev.* **2002**, *233−244*, 351–371.
(7) Gerdes, R.; Wohrle, D.; Spiller, W.; Schneider, G.; Schnurpfeil, G.; Schulz-Ekloff, G. *J. Photochem. Photobiol. A* **1997**, *111*, 65–74.
(8) (a) Ozoemena, K.; Kuznetsova, N.; Nyokong, T. *J. Photochem. Photobiol. A* **2001**, *139*, 217–224. (b) Ozoemena, K.; Kuznetsova, N.; Nyokong, T. *J. Mol. Catal. A* **2001**, *176*, 29–40.
(9) Illiev, V.; Mihaylova, A.; Bilyarska, L. *J. Mol. Catal. A* **2002**, *184*, 121–130.
(10) (a) Xu, Y.; Chen, Z. *Chem. Lett.* **2003**, *32*, 592–593. (b) Hu, M.; Xu, Y.; Xiong, Z. *Chem. Lett.* **2004**, *33*, 1092–1093.
(11) (a) Spiller, W.; Wohrle, D.; Schulz-Ekloff, G.; Ford, W. T.; Schneider, G.; Johannes, S. *J. Photochem. Photobiol. A* **1996**, *95*, 161–173. (b) Sun, A.; Xiong, Z.; Xu, Y. *J. Hazard. Mater.* **2008**, *152*, 191–195.
(12) (a) Gerdes, R.; Bartels, O.; Schneider, G.; Wohrle, D.; Schulz-Ekloff, G. *Polym. Adv. Technol.* **2001**, *12*, 152–160. (b) Hu, M.; Xu, Y.; Zhao, J. *Langmuir* **2004**, *20*, 6302–6307.
(13) (a) Xiong, Z.; Xu, Y.; Zhu, L.; Zhao, J. *Environ. Sci. Technol.* **2005**, *39*, 651–657. (b) Xiong, Z.; Xu, Y. *Chem. Mater.* **2007**, *19*, 1452–1458.
(14) He, J.; Hagfeldt, A.; Lindquist, S. E.; Grennberg, H.; Korodi, F.; Sun, L.; Akermark, B. *Langmuir* **2001**, *17*, 2743–2747.
(15) He, J.; Benko, G.; Korodi, F.; Polivka, T.; Lomoth, R.; Akermark, B.; Sun, L.; Hagfeldt, A.; Sundstrom, V. *J. Am. Chem. Soc.* **2002**, *124*, 4922–4932.
(16) O'Regan, B.; Lopez-Duarte, I.; Martinez-Diaz, M. V.; Forneli, A.; Albero, J.; Morandeira, A.; Palomares, E.; Torres, T.; Durrant, J. R. *J. Am. Chem. Soc.* **2008**, *130*, 2906–2907.
(17) Fan, F. R. F.; Bard, A. J. *J. Am. Chem. Soc.* **1979**, *101*, 6139–6140.
(18) Hodak, J.; Quinteros, C.; Litter, M. I.; Roman, E. S. *J. Chem. Soc. Faraday Trans.* **1996**, *92*, 5081–5088.
(19) Iliev, V. *J. Photochem. Photobiol. A: Chem.* **2002**, *151*, 195–199.
(20) Iliev, V.; Tomova, D.; Bilyarska, L.; Prahov, L.; Petrov, L. *J. Photochem. Photobiol. A: Chem.* **2003**, *159*, 281–287.
(21) Chen, F.; Deng, Z.; Li, X.; Zhang, J.; Zhao, J. *Chem. Phys. Lett.* **2005**, *415*, 85–88.
(22) Hong, A. P.; Bahnemann, D. W.; Hoffmann, M. R. *J. Phys. Chem.* **1987**, *91*, 6245–6251.
(23) Ranjit, K. T.; Willner, I.; Bossmann, S.; Braun, A. *J. Phys. Chem. B* **1998**, *102*, 9397–9403.
(24) Mele, G.; Garcia-Lopez, E.; Palmisano, L.; Dyrda, G.; Slota, R. *J. Phys. Chem. C* **2007**, *111*, 6581–6588.
(25) Palmisano, G.; Gutierrez, M. C.; Ferrer, M. L.; Gil-Luna, M. D.; Augugliaro, V.; Yurdakal, S.; Pagliaro, M. *J. Phys. Chem. C* **2008**, *112*, 2667–2670.
(26) Sun, A.; Zhang, G.; Xu, Y. *Mater. Lett.* **2005**, *59*, 4016–4019.

(27) Lagorio, M. G.; Dicelio, L. E.; Román, E. S. *J. Photochem. Photobiol. A* **1993**, *72*, 153–161.
(28) Iliev, V.; Mihaylova, A.; Bilyarska, L. *J. Mol. Catal. A* **2002**, *184*, 121–130.
(29) Shinohara, H.; Tsaryova, O.; Schnurpfeil, G.; Wohrle, D. *J. Photochem. Photobiol. A* **2006**, *184*, 50–57.
(30) Li, C.; Hoffman, M. Z. *J. Phys. Chem. B* **1999**, *103*, 6653–6656.
(31) Iriel, A.; Lagorio, M. G.; Dicelio, L. E.; Román, E. S. *Phys. Chem. Chem. Phys.* **2002**, *4*, 224–231.
(32) Tratnyek, P. G.; Holgné, J. *Environ. Sci. Technol.* **1991**, *25*, 1596–1604.
(33) Ingrosso, C.; Petrella, A.; Cosma, P.; Curri, M. L.; Striccoli, M.; Agostiano, A. *J. Phys. Chem. B* **2006**, *110*, 24424–24432.
(34) Janczyk, A.; Krakowska, E.; Stochel, G.; Macyk, W. *J. Am. Chem. Soc.* **2006**, *128*, 15574–15575.
(35) Stafford, U.; Gray, K. A.; Kamat, P. V. *J. Phys. Chem.* **1994**, *98*, 6343–6351.
(36) Anpo, M.; Shima, T.; Kodama, S.; Kubokawa, Y. *J. Phys. Chem.* **1987**, *91*, 4305–4310.

JP9016882